33

IFA - 95/45 Oct. 1995

AARHUS-ASTRO-1995-24 ISSN 0906-3870

FERMILAB
NOV 29 1995
LIBRARY

IFA-95-45

VARIATION IN THE SURFACE BRIGHTNESS FLUCTUATIONS OF M32

Marianne Sodemann and Bjarne Thomsen

Fermilab Library
0 1160 0049725 9

M.S.
I.D No.
NAME
RETURN TO FERMILAB LIBRARY

Inst. of Physics and Astronomy
University of Aarhus
DK-8000 Aarhus C
Denmark

To appear in The Astronomical Journal, January 1996

Variation in the Surface Brightness Fluctuations of M32 [1]

ABSTRACT

The radial behavior of B and I-band surface brightness fluctuations in M32 has been measured. We identify a systematic variation in the surface brightness fluctuations of M32, which is seen as a local minimum in the fluctuations at a distance of $R \sim 20''$ from the center. The systematic variation amounts to ~ 0.2 mag around the average value $\bar{m}_I = 22.78 \pm 0.04$, and ~ 0.3 mag around $\bar{m}_B = 26.78 \pm 0.03$. A possible population of asymptotic giant branch stars and associated post asymptotic giant branch stars likely concentrated towards the center may cause the observed increase in the luminosity fluctuations for $R < 20''$. The increase in luminosity fluctuations outward may be attributed to a possible decrease in the mean metallicity of the underlying stellar population. A comparison of the present B-band luminosity fluctuations with stellar population models having different horizontal branch morphologies indicates that a red clump horizontal branch cannot account for the observed "blue" fluctuations. During the reduction procedure the main source of contamination turned out to be a not insignificant contribution from M31's disk population. Based on the present observations and on simple simulations of the field we argue that the mere recovery of added stars does not necessarily guarantee that the derived stellar photometry represents the true photometric properties of the stellar population. Realistic simulations of the crowded field are essential in order to select a criterion that will eliminate spurious sources due to the surface brightness fluctuations. Simulations show that our ground-based images with $\sim 1''.0$ seeing do not have the spatial resolution that will allow us to supplement the fluctuation measurement with stellar photometry of the most luminous stars.

---

[1] Based on observations obtained with the Nordic Optical Telescope, La Palma.

1. Introduction

This paper is a continuation of a project dealing with the radial behavior of surface brightness fluctuations (SBF) in elliptical galaxies. The idea behind utilizing the SBF was introduced by Tonry & Schneider in 1988 as a new technique for measuring extragalactic distances, and, potentially, as a probe of stellar populations. In the search for both a calibration of $\bar{M}$ versus stellar population, and for a better understanding of stellar populations, many measurements of SBF have been made (e.g., Tonry 1991, Ahjar & Tonry 1994). Tonry (1991) presented a radial gradient of the SBF in the Local Group galaxy NGC 205, a companion galaxy to M31. A procedure for measuring the radial behavior of SBF was presented in Sodemann & Thomsen (1995) (hereafter referred to as ST). Based on observations of NGC 3379, ST demonstrated that it is possible to measure radial changes accurately. The procedure takes into account that unwanted point sources such as foreground stars, background galaxies, and globular clusters are located in a background of varying amounts of luminosity and photon fluctuations. In this paper we apply the same procedure to M32 (=NGC221), another of M31's four companion galaxies. The main source of contamination to the luminosity fluctuations measured for M32 turn out to be a contribution from the M31 disk stars, in addition to a very small contribution from the galactic foreground stars and background galaxies.

M32 is a compact elliptical galaxy with very high central surface brightness. It resembles giant ellipticals in the sense that M32 represents the low-luminosity extension of the classical giant elliptical galaxy family (Ferguson & Binggeli 1994, Freedman 1992a, Peletier 1992). Though being a low-luminosity elliptical, M32 is not structurally different from the normal giant ellipticals (Kormendy 1985). However, contrary to what could be expected from its total magnitude $M_V = -16.3$, M32 carries no known globular clusters of its own (Harris 1991). In a HST study of the cores of elliptical galaxies M32 is found to belong to the group of unresolved low-luminosity ellipticals (Kormendy *et al.* 1994). There was no sign that M32 should be unusually compact. Faber (1973) proposed that M32 could be the central dense remnant of a tidally stripped normal elliptical. The present day M32 may then be the old remnant, which withholds some of the original giant-like properties, together with a younger intermediate-age population for which there is strong evidence, see below. Peletier *et al.* (1990) showed that the lowest luminosity galaxies in their sample of ellipticals have small or zero gradients. As other compact ellipticals M32 does not display significant optical color gradients (Freedman 1992a, Peletier 1993, Michard & Nieto 1991). From near-infrared imaging Silva & Elston (1994) concluded that the color profiles of M32 were essentially flat and consistent with Peletier (1993). Besides that M32, like NGC 3379, is a fiducial galaxy for the investigation of the radial behavior of SBF in elliptical galaxies,

it is one of the important galaxies for calibration of the SBF.

The SBF of a galaxy depend on the composition of the underlying stellar population. For the distance measurements, this dependence is sought calibrated through the known broad-band color of the galaxy. Tonry (1991) calibrated $\bar{M}_I$ against the integrated color $V - I$ by adopting a distance to M31 and M32 of 0.77 Mpc (Freedman & Madore 1990) for the zero point, and the slope of ~ 3 was based on Local Group galaxies and the Fornax and Eridanus cluster (see also Ahjar & Tonry 1994). As outlined in ST, the linear relationship between $\bar{m}_I$ and $(B - I)$ found for NGC 3379 was a reassurance for the calibration adopted by Tonry (1991). However, the difference between the integrated color and the color of the surface brightness should be borne in mind. Whenever a significant color gradient is present the integrated color will deviate from the color of the surface brightness. Moreover, we believe that it is physically most correct to compare the *local* SBF magnitude $\bar{m}$ with the *local* surface brightness color. This distinction is not a serious matter for M32, which does not show signs of significant broad-band color gradients.

Freedman (1992b) resolved an off-nuclear extended giant branch population in M32 interpreted as intermediate-age asymptotic giant branch (AGB) stars. The identified AGB stars are supposed to be the giant star successors of high-mass intermediate-age dwarf stars. This indicated that M32 had an episode of star formation ~ 5 Gyr ago. The evidence of an extended giant branch in M32 was presented in several studies in 1992, see Davidge & Jones, Davidge & Nieto, and Elston & Silva. From optical spectroscopy of the nucleus of M32 O'Connell (1980), Burstein *et al.* (1984), and Rose (1985) found evidence for an intermediate-age population, but this hypothesis is not universally accepted (Renzini 1986). The central metallicity of M32 is by O'Connell inferred to be near solar. Also based on optical spectroscopy Hardy *et al.* (1994) inferred the presence of an intermediate-age stellar population in M32. Whereas a radial gradient in the Mg_2 feature was identified, they found no evidence for a radial variation in either age or the Fe/Mg ratio. The radial variation in Mg_2 was transformed into a metallicity gradient of $\Delta[\mathrm{Fe/H}]/\Delta \log(R) = -0.25 \pm 0.07$ ($15'' < R < 60''$). This is not significantly different from the findings for giant ellipticals (Davies *et al.* 1993, and references therein). As Hardy *et al.* noted, Davidge (1991) failed to see this gradient in Mg_2, probably due to the fact that the study was confined to the central plateau ($R < 25''$). It has been known for a long time that M32 shows enhanced nuclear H_β absorption compared to galactic globular clusters indicative of a young population (Burstein *et al.* 1984, Faber *et al.* 1992, Faber *et al.* 1995). In the data of Davidge (1991) a radial weakening of both the H_β and the H_α index was seen. Hardy *et al.* (1994) identified a radial strengthening in H_α, i.e. line width decreasing towards the center of M32. Since H_β showed to be approximately constant, the variation in H_α was attributed to a presence of a diffuse emission component concentrated towards the center. They stressed doubts about

H_β as a population diagnostic in M32. Imaging of a field located $\sim 2'$ to the south-east of the center of M32 showed evidence for both age and metallicity gradients (Davidge & Jones 1992). The issue of H_β as a "young population" tracer is controversial. As outlined by Burstein *et al.* (1984) there are other stellar components that might explain the Balmer-line enhancements: a hot horizontal branch and blue stragglers.

Based on the inferred population of AGB stars in M32 we have initiated a series of simulations, which will show to what degree a detection of the AGB population depends on seeing conditions and crowding. Indeed, whenever a galaxy is too distant, or a field too crowded (say, the center of M32), we are unable to sample individual stars, and we turn to measurements of the average galaxy light, and the variance of the galaxy light, i.e. measurements of the luminosity fluctuations. Our preliminary results regarding this problem for M32 will be discussed in Sec. 3. The effects of seeing and crowding in imaging of M32 are also discussed by DePoy *et al.* (1993).

Besides the above mentioned indices, broad-band colors, and spectral line indices, the luminosity fluctuations of a galaxy are believed to reveal new information on the stellar population (e.g., Ajhar & Tonry 1994). Our knowledge about the galaxies obtained from colors and line strengths is to a large degree still dominated by the unknown effects of e.g. age and metallicity. The investigation of the radial behavior of SBF in NGC 3379 showed that the I-band luminosity fluctuations are sensitive to local changes in the underlying stellar population, whereas the new information derived was correlated with the broad-band color $B - I$ (ST). In a recent paper Jones & Worthey (1995) have presented a Balmer line index, which is sensitive almost exclusively to age. This news indicates that the index is able to disentangle the degeneracy between age and metallicity in stellar populations. However, the Jones & Worthey result is based on a grid of single-age and single-metallicity models (the same models to which we shall compare our observations). It is unclear if the new Balmer line index is able to disentangle the degeneracy between age and metallicity in real composite populations. Other possible population characteristics than age and metallicity will be discussed in Sec. 5.

Regarding the SBF, we adopt the nomenclature present in ST, which is very nearly identical to that presented in the original paper on SBF (Tonry & Schneider 1988). Due to the discreteness of the stars, Poissonean statistics apply to the number of stars N per pixel, where the description for simplicity is restricted to only one type of stars. The variance of the galaxy flux normalized by the average galaxy flux then is $\bar{f} \equiv \tilde{\sigma}_{\rm L}^2 = \sigma_{\rm L}^2/\bar{g}$. Here $\bar{g} = \bar{N}\bar{f}$ is the average galaxy flux per pixel, and $\bar{f}$ is the flux weighted average flux of each star, measured in ADU's or given as the magnitude $\bar{m}$. The contribution to the SBF signal $\bar{f}$ from sources not belonging to M32 is dealt with in Sec. 3. The flux $\bar{f}$ is

measured in the Fourier power spectrum of the luminosity fluctuations as described in Sec. 4. The interpretation of the radial behavior of the SBF will be discussed in Sec. 5 in relation to properties of M32 found by others, and we will compare our observations with the state-of-the-art stellar population models of Worthey (1993, 1994).

2. Observations and Data Reduction

2.1. Basic Reductions and Calibration

The data presented here were obtained on the 1st of September 1994 with the 2.5 m Nordic Optical Telescope, La Palma. The exposures consist of 9×25 s in I ($\sim$ 7900 Å) and 11×90 s in B ($\sim$ 4400 Å). They were obtained using a TEK-1024 CCD (gain 3.3 e^- per ADU, readout noise 2.0 ADU) at the f/11 Cassegrain focus, which yielded pixels of 0.″175 on the sky and a well-sampled point spread function (PSF). The seeing in the images was near 1.″0 FWHM in both I and B. Before preparing the images for the SBF analysis, the basic reductions were carried out in the usual way. An average bias frame and an individual residual bias level were subtracted, and the images were flat-fielded by high signal twilight flats. From series of rotated flat-fields we detected no indications of scattered light. A technical engineering test showed no non-linearity effects in the detector.

Within an aperture of radius 11.″2 centered on the galaxy we have compared the flux derived from exposures (with approximately the same seeing) taken throughout the night. This revealed that the weather was photometric, and the atmospheric extinction coefficients obtained were $k_B = 0.21$ and $k_I = 0.05$ mag per airmass. The range in airmass for these exposures was 1.0 – 1.4. For that particular night Morrison (1994) informed that $k_V = 0.14$, obtained with the Carlsberg Automatic Transit Circle. With this value of k_V it was possible also to calculate the values of k_B and k_I (King 1985). The observed and predicted values of k_B and k_I agree within a few hundredths of a magnitude. The standard colors as a function of instrumental colors for the sample of standard stars form a straight line with slope 1.05 and dispersion 0.02. This means that the difference between the effective wavelengths of the B and I passband for the applied filters is only 175 Å smaller than for the standard system.

Standard stars were observed twice during the night. They consist of standard stars in the galactic globular cluster M92 and Landolt standard stars (Landolt 1992). Calibrations of M92 were made using the B-band photometry of Stetson & Harris (1988) and unpublished I-band photometry of Davis (1995) (see also Majewski *et al.* 1994). The slightly defocused standard stars were measured by DAOPHOT II's routine PHOTOMETRY (Stetson 1987).

The magnitudes belonging to an aperture of radius 2.″6, which extended well outside the defocused part of the stellar profiles, turned out to have the smallest internal scatter, and they were hence used as basis for our stellar photometry. A mean growth curve was determined for each exposure and the small aperture (radius = 2.″6) photometry of the standard stars was corrected to a larger standard aperture of radius 5.″2 that was supposed to contain nearly all of the stellar flux. This aperture size was used when we transformed the instrumental magnitudes of the PSF star to the standard system. However, we had to adopt a much larger standard aperture of radius 21″ for the aperture correction, when we were dealing with the I-band photometry of the galaxy. We discovered that the I-band stellar profiles had unusual broad wings, which is evident in Fig. 1. In such a situation the adopted aperture correction must be based on the scales of the object under consideration. Capaccioli & de Vaucourleurs (1983) described a re-distribution of light from the brighter parts into the external regions as due to scattering by dust on the mirror, atmospheric haze, and inhomogeneities in the combined optical system (i.e., telescope, filters, detector). For the B-band photometry of the galaxy the standard aperture was set to a radius of 7.″0, since the effect of re-distribution of light turned out to be much less pronounced in B. The difference in airmass between the M92 standard stars and the standard stars of Landolt, and between the standard stars and M32, were corrected for by applying the extinction coefficients derived above. Two of the twelve standard stars covered the color of M32, and color terms are at most 0.04. We have obtained a photometric accuracy for the standard stars of 0.03 in I and 0.02 in B.

The exposures, 9 in I and 11 in B, where observed within 30 min and 45 min, respectively. The background (sky+M31), which varied less than 1 ADU among each set of exposures, was determined in the following way (see also Sodemann & Thomsen 1994). From an exposure reaching out to $\sim$ 3.′7 from the nucleus of M32 to the south-east we adopted a first estimate of the background. With this value of the background we estimated

Fig. 1.— I-band growth curve for one bright relatively isolated calibrating star in M92. This clearly demonstrates the effects of light scattered from the central parts of the stellar object into the wings. Plotted is the integrated magnitude within 12 different radii subtracted from the integrated magnitude within the innermost aperture of radius 2.″6. The standard aperture adopted for aperture correction in the I-band had a radius of 5.″2 when dealing with the photometry of the PSF and a radius of 21″ when dealing with the photometry of the galaxy. Neighboring stars were masked out in order to determine a background not too affected by point sources. The inner and outer sky annuli were 38″ and 45″, respectively. The PHOTOMETRY routine of DAOPHOT II was applied (Stetson 1987).

the contribution from the galaxy in the region overlapping the exposure with the galaxy center. In this way we had an estimate of the background in the exposure with the galaxy center, and this value only had to be adjusted by a few ADU in order to obtain a straight surface-brightness profile in the outer parts of the galaxy, assuming an $R^{1/4}$ dependence. This assumption was based on a comparison of different $R^{1/n}$ profiles with the observed profile (Caon *et al.* 1993; see also Tonry 1984), and any systematic error introduced by the background removal is completely covered by the statistical error. We have tacitly assumed that the contribution from M31 to the background did not vary over the range of $\sim 3\farcm7$ from the center of M32 to the south-east. After registering to a common center, cosmic ray events were removed by taking the median of each of the two sets of selected exposures. This reduced the level of white noise in a predictable way. By simulations we determined the effective gain in each of the combined images.

To test our calibration of M32 we have compared our aperture photometry with that of Burstein *et al.* (1987) and Sandage & Visvanathan (1978). The integrated $B-I$ color is compared with the colors found by Peletier (1993) (hereafter referred to as P93) and Gregg (1989), see Table 1. Since there are no significant color gradients present in M32, we may for this galaxy directly compare integrated colors with the color of the surface brightness as presented in P93. Our photometry in B is within the errors of the photometry by Burstein *et al.* and Sandage & Visvanathan. Our integrated color is in agreement with the findings of P93 and Gregg. Within the measurement errors our galaxy profiles are in agreement with those of P93 in the range $10'' < R < 40''$. Inside $\sim 10''$ our profiles are unreliable due to the effects of scattered light as discussed above. Outside $\sim 40''$ the profiles of P93 are dominated by the background due to the way the profiles were created.

We shall later in this paper compare our results of SBF in M32 with the results presented in Tonry *et al.* (1990) and with our results for NGC 3379 (ST), and we correct for galactic absorption. There is strong evidence that M32 is not situated behind but in front of the M31 disk (Freedman 1989), and internal absorption in M32 is not expected. We adopted $A_B = 0.31$ (Burstein & Heiles 1984), where $A_B = 4 \times E(B-V)$. Using the extinction law available in Cardelli *et al.* (1989) we found $A_I = 0.14$, taking into account that the effective wavelength of our I-band was close to that of Cousins. This implied a color excess of $\mathrm{E}(B-I) = 0.17$.

2.2. Preparation for SBF Analysis

We are now in possession of two images from which we want to extract and measure the SBF. The luminosity fluctuations emerge when a smooth fit to the image, that is

M32+background, is subtracted. The smooth fit was obtained by applying our galaxy fitting routine, which is described elsewhere (Sodemann & Thomsen 1994), and the two residual images with the luminosity fluctuations were then subjected to further analysis. The total radial range in each image covered $7''.0 \leq R \leq 50''.7$. In order to investigate the radial behavior of SBF in M32 this annulus was divided into five subannuli: (A1) $8''.0 \leq R < 14''.8$, (A2) $16''.8 \leq R < 23''.6$, (A3) $25''.5 \leq R < 32''.3$, (A4) $34''.2 \leq R < 41''.1$, and (A5) $43''.0 \leq R \leq 49''.8$. Each radial range defines a mask, which equals one inside the defined range. Outside the range it is described by a Gaussian fall-off to zero with dispersion equal to five pixels. Such "soft" window masks suppress discontinuities and prevent leakage of power from low to high wavenumbers, which is especially important for the I-band image where the fluctuation signal is a factor of several hundred above the white noise level (Press *et al.* 1992).

3. Point Source Photometry

Before a reliable measurement of the SBF in M32 can be carried out, all unwanted contaminating point sources have to be extracted from the residual images. For an isolated galaxy these point sources are galactic foreground stars, globular clusters, and background galaxies embedded within the luminosity and photon fluctuations. Since M32 is situated just in front of the M31 disk, we also examine the possible influence from M31 on the measured variance of M32. Any contribution from globular clusters (GCs) in M32 is precluded since M32 has no globular cluster system of its own (Harris 1991). In case GCs were present in the images they would appear resolved with diameters of $\sim 5'$ (Racine 1991). No such non-stellar objects are apparent in our images. Any presence of resolved GCs can then be rejected in the following way. If we adopt $M_V = -7.6 \pm 0.15$ for the top point of the globular cluster luminosity function (GCLF) and $m_V - M_V = 24.6$ (Reed *et al.* 1994), and take $(B - V) = 0.7$ and $(B - I) = 1.9$ as typical colors of the GCs (Reed *et al.* 1994, Ahjar & Tonry 1994), then we would expect the apparent magnitude of the GCLF top point for M31 to be at approximately $m_I = 15.8$, or $m_B = 17.7$, where our data are 100% complete. This implies that the identification of unwanted point sources is reduced to an elimination of foreground stars, background galaxies, and disk stars of M31, and a correction for their residual variance.

Identification and photometry of the point sources were performed by employing the photometry package DAOPHOT II (Stetson 1987). In ST [see equation (1) therein] we introduced a slight modification of ALLSTAR. As described in ST we incorporate the normalized amplitude of the combined luminosity and photon fluctuations as a better estimate of the noise map than ALLSTAR's original one, which is based on photon noise

only. The PSF used by ALLSTAR during the fitting process was defined by DAOPHOT using one bright unsaturated isolated star from the I and B image, respectively. The magnitude of the PSF is $m_I = 14.40$, and $m_B = 16.13$. This PSF is also the PSF employed during the measurement of the luminosity fluctuations described in Sec. 4.

The discrimination between real point sources and spurious sources due to luminosity and photon fluctuations was based on simulations of the latter as described in the following (see ST for details). A preliminary measurement of the luminosity fluctuations for the whole area ($7\farcs0 \leq R \leq 50\farcs7$) of the residual images gave $\bar{f}_I = 39.2$ ADU per star per 25 sec, and $\bar{f}_B = 6.8$ ADU per star per 90 sec. Applying ALLSTAR to the simulated luminosity fluctuations provided a lower limit in SIGMA (the uncertainty of the associated magnitude as calculated by ALLSTAR) for spurious detections. This limit of SIGMA was 0.04 in I, and 0.03 in B (the limits did not vary significantly between the individual annuli). With the lower limits in SIGMA, we were able to separate the luminosity and photon fluctuations from the real point sources, which have more well-determined magnitudes. This resulted in a total of five point sources, that all have bluer colors than M32. If a distance modulus of ~ 24.4 is adopted for M31/M32 (Tonry 1991), the absolute magnitudes of the detected point sources are similar to those of very luminous early-type stars. However, no dust lanes or associations are visible in the images (see also Freedman 1989), so we can neither associate these blue objects with M31 nor with M32. We identify the five point sources as galactic foreground stars, the faintest having magnitude $m_I = 18.50$, and $m_B = 19.64$. M32 has the galactic coordinates $(l, b) = (121\fdg15, -21\fdg98)$ (de Vaucouleurs *et al.* 1991), and the number of identified foreground stars in this field is in agreement with the number predicted by Ratnatunga & Bachall (1985).

The final mask, which was applied to each of the two residual images, was the mask removing the five point sources multiplied by a mask defining the region of interest according to the five annuli (Sec. 2.2). However, we cannot necessarily expect our elimination of contaminating point sources to be complete. The incompleteness of our detection procedure was tested in the same way as described in ST by adding and retrieving stars (scaled PSFs) using the ADDSTAR routine of DAOPHOT. The test was carried out for both the I and B-band, and all spurious sources detected were eliminated using the limits of SIGMA derived above. The test showed that the limiting B-band magnitude at half probability was $m^B_{1/2} = 21.8$ for the innermost annulus (A1), and $m^B_{1/2} = 22.4$ for the outermost annulus (A5). The limiting I-band magnitude at half probability was $m^I_{1/2} = 19.3$ (A1), and $m^I_{1/2} = 19.9$ (A5). Knowing the degree of incompleteness we could then, as outlined next, calculate estimates of residual variances from point sources not excised by the mask.

To estimate the contribution to the B-band luminosity fluctuations from faint

foreground stars (fgs) in our own galaxy we adopted a power-law luminosity function $n_{\rm fgs} = N_0 10^{r(m-m_0)}$, where N_0 is the number of foreground stars per magnitude at $m = m_0$. We considered only magnitudes larger than the faintest point source $m_0 = 19.64$. The slope r was estimated from the star count data of Bahcall & Soneira (1980) for magnitudes faintward of $m_B \sim 20.0$ giving $r = 0.07$. We were then able to apply the equations (7) – (10) in ST and thereby estimate the residual contribution from foreground stars in each annuli. The normalized variance for the individual annuli turned out to be less than 0.1 ADU per 90 s in B, i.e., measured in magnitudes the correction for galactic foreground stars faintward of $m_B = 19.64$ was less than 0.01 and regarded as negligible. A contribution from faint foreground stars relatively to luminosity fluctuations are even less for the more powerful I-band fluctuations. It also turned out that the depth of the images only reach magnitudes where the residual variance from background galaxies is vanishing. The galaxy counts of Tyson (1988) predict only one to two galaxies within our images, and visual inspection of the images indicates that no background galaxies are present. The number of background galaxies obey a similar power-law luminosity function as the foreground stars with slope $s_I = 0.32$ and $s_B = 0.45$ (Lilly *et al.* 1991, Tyson 1988). Applying the equations (7) – (10) in ST showed that the correction for residual variance from background galaxies in I and B, respectively, was less than 0.01 magnitudes. These small parts of the measured variance were regarded as negligible, and the measured power $P_0^{I,B}$ of the SBF (Sec. 4) is expressed as the magnitudes $\bar{m}'_{I,B}$.

From the following argument it may be seen that luminosity fluctuations from stars in the M31 disk are not insignificant. Afterwards we shall apply an approximate correction. The measured SBF signal in the B-band amounted to $\bar{f}_B \sim 6$ ADU during 90 s, which corresponds to $\bar{m}_B \sim 27$. Objects in M31 with this apparent magnitude would have $M_B \sim 2.5$, which is expected to be a typical magnitude of an F dwarf in the M31 disk. So, M31 may contribute to the measured fluctuation signal, and we correct for that part of the SBF signal as described next. The effect of M31 was sought furthest from the center of M32, that is, in a square in the most north-westerly part of the residual image. The square was chosen to have approximately an area similar to that of the outermost annulus. The choice of a position close to M31 provided an upper limit to the local influence from M31 relative to M32. The square is situated just at the edge of the A86 Hodge association (Hodge 1981), also outlined and labeled in Fig. 1 of Freedman (1989). As for each annulus centered on M32 the measured variance $\sigma^2_\square$ in the square is the sum of luminosity fluctuations in M32 and M31. Assuming that the influence from M31 is constant over the field studied, the contribution from M31 to the luminosity fluctuations cancels when $\sigma^2_\square = \bar{f}_\square \bar{g}_\square + \sigma^2_{\rm M31}$ is subtracted from the measured variance $\sigma^2 = \bar{f}\bar{g} + \sigma^2_{\rm M31}$ of each annuli. $\bar{g}$ and $\bar{g}_\square$ are the average fluxes of M32 in the annulus and in the square, respectively. The power of the

luminosity fluctuations was measured by our filtering technique (Sec.4). The normalized fluctuation signal then takes the form $\bar{f} = (\sigma^2 - \sigma^2_{\square})/(\bar{g} - \bar{g}_{\square})$, if $\bar{f} \approx \bar{f}_{\square}$ is assumed. With this estimate of $\bar{f}$ we avoid any assumption on the background level, and any previous estimates of the background are therefore automatically adjusted. The effect from M31 in B was typically an increase in the fluctuation signal of 5%, and the measured fluctuation signal $\bar{m}'_B$ was corrected accordingly. In I the effect was at most a decrease of 5% and the signal $\bar{m}'_I$ was corrected (mainly adjustment of background). This resulted in the magnitudes $\bar{m}_I$ and $\bar{m}_B$ given in Table 2. Note that the adopted square in the residual images serves as a 'control area' and the procedure just described had covered a correction for foreground stars and background galaxies in case their influence had not been insignificant.

Caution must be exercised when simulating the luminosity fluctuations of M32. The number of stars per pixel (estimated by $\bar{g}/\bar{f}$) is reduced from about 18 in the innermost annulus down to 2 in the outermost annulus, whereas for NGC 3379 the numbers are 445 and 54 respectively. With the low number of stars per pixel for M32 it may no longer be sufficient to simulate the SBF by a Poissonean distribution of stars with the same flux $\bar{f}$. In other words, whenever the resolution of individual stars improves, more information than simply the fluctuation amplitude may tend to emerge from the observations. Such additional information could be a reliable detection of individual bright stars, which would likely stand out in a histogram of all detected objects (both real and spurious). In order to test this we have compared the residual I-band image with simulations based on a luminosity function which equals a delta function at $\bar{f}$, corresponding to $\bar{m}_I = 22.78$. (By applying the filtering technique as described in Sec. 4 to the simulated image of SBF, we of course retrieve the flux $\bar{f}$.) In this test DAOPHOT was forced to find all objects above a threshold of 2.0 standard deviations of the sky level (as derived by DAOPHOT). The total number of objects with magnitude $I < 20$ was 381 for the simulated image and 380 for the real image. For $20 < I < 21$ we found 911 and 820 objects for the simulated and real image, respectively. In case the simulations were inappropriate for M32 we would expect clear differencies in the distributions of the objects in Fig. 2, where the data have been binned into histograms.

In Fig. 2 all objects with SIGMA larger than 0.08 were eliminated in order to pick out the objects with the most well-determined magnitudes. The cut-off in the bulk of objects for $I > 19.5$ is due to incompleteness. Regarding $I < 19.5$ (and ignoring the few bright foreground stars), the distribution of observed objects in the present data is apparently not different from the distribution of spurious sources found by ALLSTAR in the simple simulations. Therefore, based on the present observations and the application of ALLSTAR we conclude that it is not possible to distinguish between individual bright stars and the luminosity fluctuations, i.e., we are not able to make further predictions on the underlying

luminosity functions. This conclusion is not altered by a change from 2.0 to 9.0 standard deviations of the threshold in DAOPHOT's FIND routine, which reduces the total number of objects by approximately a factor of four. This implies that the similarity between the real and simulated image is not caused by DAOPHOT's star-detection threshold. If the lack of differencies between the real and the simulated image is not introduced by possible differencies in the application of ALLSTAR as compared to NSTAR, we are inclined to suggest that a fraction of the supposedly resolved central AGB population studied by Davidge & Nieto (1992) may indeed be luminosity fluctuations. The effect of luminosity fluctuations on the photometric properties of a population of bright stars is of course influenced by the seeing conditions present. The influence from seeing and/or crowding effects must be carefully examined by simulations of the observed field. More realistic simulations than those described above are being carried out (Thomsen & Sodemann 1995). They involve appropriate populations of both red giant branch (RGB) stars, and main sequence stars. We examine histograms like Fig. 2 of the retrieved stars and the luminosity fluctuations in order to see how seeing effects influence the identification of the tip of the RGB (and thereby a possible identification of an AGB population). Our very preliminary results show that if the present observations had been made with 0.″5 seeing, the tip of the RGB would tend to emerge from the luminosity fluctuations. At this stage we merely emphasize the following: completeness tests (i.e., addition and retrieval of individual stars) are necessary, but not sufficient, when trying to extract HR diagrams and luminosity functions for the detected objects in an observed field. The completeness tests must be accompanied by simulations of the observed field and include a criterion that can seperate false detections from real point sources. The contribution from AGB stars to the luminosity fluctuations will be discussed in Sec. 5.

As mentioned above, the effect of incompleteness is seen in Fig. 2 as the decrease in number of objects faintward of $I \sim 19.5$. A simple qualitative argument can explain why the identified objects turn up at magnitudes much brighter than the magnitude $\bar{m}_I = 22.78$ for a single object (presented as the vertical line in Fig. 2). Neglecting details about how ALLSTAR treats individual objects, and assuming that all stars have the same flux $\bar{f}$,

Fig. 2.— Histogram of detected objects in the original I-band residual image (full line), and of detected objects in the simulated image where the luminosity function equals a delta function at $I = \bar{m}_I = 22.78$ (dashed line). All detected objects with SIGMA larger than 0.08 have been eliminated, see text. The data are plotted in 0.1 magnitude bins. The vertical line represents the average magnitude of a fluctuation star with $I = \bar{m}_I$. The gap between $I \sim 19.5$, where the bulk of objects is found, and $I = 22.78$ is explained qualitatively in the text. Data are 100% complete for $I < 19.5$

corresponding to $\bar{m}$, the argument goes as follows: We now consider the number of stars per resolution element $N_\circ$ with the average $\bar{N}_\circ$. The actual flux from a specific resolution element is $N_\circ \bar{f}$, whereas the average flux from stars in adjacent resolution elements is $\bar{N}_\circ \bar{f}$. A flux enhancement above average then is $\Delta f = (N_\circ - \bar{N}_\circ)\bar{f}$, and the corresponding magnitude offset of the positive fluctuation is $\Delta m = 2.5 \log(\Delta f / \bar{f}) = 2.5 \log(N_\circ - \bar{N}_\circ)$. This implies that a statistical event such as 20 stars above average per resolution element would be measured as a lump of fluctuation stars with magnitude $2.5 \log(20) = 3.3$ brighter than the neighboring resolution elements. For the innermost and outermost annuli we have an average of approximately 500 and 60 stars per resolution element respectively. Applying the Poisson distribution with those parameters it is easy to show that for the outermost annulus only $\sim 1\%$ of the resolution elements will have enhancements of 20 stars above average, whereas for the innermost annulus $\sim 20\%$ of the resolution elements will give rise to enhancements seen 3.3 mag brighter than $\bar{m}$. This merely shows that it is indeed possible for DAOPHOT/ALLSTAR to identify and measure such lumps of fluctuation stars as a single spurious star that is much brighter than $\bar{m}$.

4. Measurement of SBF

As was emphasized in the original paper on SBF (Tonry & Schneider 1988) the key to the method is the spatial power spectrum of the luminosity fluctuations. During a Fourier transform white noise separates from the luminosity fluctuations, which have the PSF impressed upon them, and the analysis and measurement of SBF is therefore carried out in the Fourier domain. The variance of the luminosity fluctuations is obtained by the filtering technique introduced in ST.

The residual images are divided by the square root of the average galaxy flux per pixel for I and B, respectively. We now seek the normalized luminosity fluctuations $\bar{f} \equiv \tilde{\sigma}_{\rm L}^2 = \sigma_{\rm L}^2 / \bar{g}$. The power of the luminosity fluctuations is $P_0 = \tilde{\sigma}_0^2$ (measured in ADUs), which is the sum of the sought amplitude of the luminosity fluctuations $P_{\rm L} = \tilde{\sigma}_{\rm L}^2$ and the contribution from the M31 disk population. The level of white noise in the power spectrum is given by $P_1 = \tilde{\sigma}_{\rm N}^2 = \sigma_{\rm N}^2 / \bar{g}$ [Eq. (12) in ST]. The appearance of the Fourier transform of the normalized residual image is governed by the Fourier transform of the PSF present in the image. The adopted form of the Optical Transfer Function (OTF) is (Thomsen & Frandsen 1983)

$$OTF(u,v) = a\, H(\omega) \exp(-2\pi \mathrm{i} \theta)$$

$$\theta = \alpha\, u + \beta\, v$$

$$H(\omega) = \exp(-(\omega/\gamma)^n) \tag{1}$$

$$\omega^2 = u^2 + v^2 + a_2\,(u^2 - v^2) + 2\,b_2\,u\,v\,,$$

where $OTF(0,0) \equiv 1$. This functional form with $n = 1.64$ was an excellent fit at all wavenumbers to the PSF present in ST. However, Eq. (1) cannot for a given value of n simultaneously fit the inner and outer parts of the Fourier transform of the present PSF, due to the PSF's unusual broad wings (Sec. 2.1). We deal with this by measuring the power of *both* the luminosity fluctuations *and* the PSF. This provides a measurement $\bar{m}$ of the luminosity fluctuations, which is an off-set in magnitude relative to that of the PSF. In this way the measurement of the luminosity fluctuations is basically dependent on the photometric calibration of the PSF and insensitive to the small departure between the empirical and the analytical OTF at small wavenumbers. Our filtering technique is described below, and the power spectra are shown in Fig. 3.

From the two-dimensional power spectra of the residual images and their corresponding PSF's we calculate radial profiles $P(\omega)$ of average pixel values in the power spectra as a function of the radial wavenumber coordinate ω. We take into account the ellipticity of the OTF. The width of the elliptical rings is 1 pixel, and $nop(\omega)$ denotes the number of pixels in each ring. Seeking the power of the luminosity fluctuations we are interested only in the power at small wavenumbers, that is, the wavenumbers where the power spectrum is dominated by the OTF and not the wavenumbers at or beyond the transition to the region where the power spectrum is dominated by white noise. We therefore made the fit of the analytical OTF to the Fourier transform of our PSF at small wavenumbers $\omega \leq 130$. This resulted in $n = 1.34$ for the B-band PSF and $n = 1.22$ for the I-band PSF. The PSF was extracted from the residual image by applying a mask that covered the area of the standard aperture (Sec. 2.1) and had a diameter corresponding to the width of the subannuli (Sec. 2.2). From the analytical $OTF(\omega)$ we define the low-pass filter $|OTF(\omega)|^4/(|OTF(\omega)|^4 + P_1^2/P_0^2)$, which takes into account the ratio of white noise to fluctuation power. The level of white noise is subtracted from the power of the residual

Fig. 3.— Power spectra of normalized luminosity fluctuations, one for each annulus in I (ADU per 25 s) and B (ADU per 90 s), respectively. Also shown is the sum of the power P_0 times $|OTF(\omega)|^2$ plus the level of white noise P_1. The luminosity fluctuation signal $\bar{f}$ is derived from the power spectrum with wavenumbers in the range $25 \leq \omega \leq 130$, corresponding to the central few arcsec ($\sim 1'' - 7''$) of the PSF.

image and the difference is divided by $|OTF(\omega)|^2$. Applying the low-pass filter the estimate of the power P_0 becomes:

$$P_0 = \frac{\sum_\omega nop(\omega) \frac{|OTF(\omega)|^4}{|OTF(\omega)|^4 + P_1^2/P_0^2} (P(\omega) - P_1)/|OTF(\omega)|^2}{\sum_\omega nop(\omega) \frac{|OTF(\omega)|^4}{|OTF(\omega)|^4 + P_1^2/P_0^2}} . \quad (2)$$

Only a few (two to three) iterations were needed before convergence. The wavenumbers, for which the filter was applied, ranged from 25 to 130 (corresponding to $\sim 1'' - 7''$). Wave numbers $\omega < 25$ (corresponding to scales larger than $7''$) were avoided due to the effects of the galaxy fitting routine, which for the innermost annuli depresses large scale structures. Applying the galaxy fitting routine to an image of simulated SBF and measuring the fluctuation power of the residual image in the range $25 \leq \omega \leq 130$ show that the fluctuation measurement is not systematically affected by the fitting routine.

As emphasized above we apply Eq. (2) to the power of both the luminosity fluctuations and the PSF. In Table 2 we present the estimated power of the luminosity fluctuations P_0^B and P_0^I as a function of the geometric mean radius R of each annulus. Via the estimated power of the PSF we arrive at the magnitudes $\bar{m}'_{I,B}$, which were corrected for the effect of the M31 disk population resulting in the magnitudes $\bar{m}_{I,B}$. Correction for galactic reddening has been applied to all magnitudes $\bar{m}'_{I,B}$ and $\bar{m}_{I,B}$ in Table 2. An application of Eq. (2) to a series of images with simulated SBF showed that the statistical error introduced amounts to at most 0.02 magnitudes. The total statistical error from the photometry and the filtering technique then is 0.04 magnitudes in I and 0.03 in B.

5. Discussion

Radial stellar population gradients exist in many elliptical galaxies, and the search for a proper interpretation of the radial properties is a challenging task. The present investigation of the radial behavior of SBF in M32 may be considered as a contribution to the knowledge of our closest elliptical galaxy. Table 2 contains the data of our radial analysis. In Fig. 4 the measured fluctuation signals $\bar{m}_I$ and $\bar{m}_B$, and the color $\bar{m}_B - \bar{m}_I$, are presented, and the stellar population model data of Worthey (1993, 1994) are superposed. As may be evident in Fig. 4 the observed $\bar{m}_I$ and $\bar{m}_B$ for the five distinct annuli vary in a systematic way. The variation in luminosity fluctuations in both I and B may be described as an upturn towards the center and an upturn outwards with an apparent minimum at $R \sim 20''$. The remainder of this paper is mainly dealing with the ongoing discussion of age and metallicity effects, and additional characteristics of stellar populations.

The spectroscopy by Hardy *et al.* (1994) emphasized the existence of a radial gradient in Mg_2, but an upper limit of 3 Gyr for any possible age gradient within $2r_e$. They showed that the mean spectral energy distribution of M32 could not be matched by any globular cluster spectra, or by any combination of them, whereas a good fit was obtained when intermediate-age clusters were allowed into the spectral mix. Their observed gradient in Mg_2 covered $15'' \leq R \leq 60''$ and was found to correspond to $\Delta[\mathrm{Fe/H}]/\Delta \log(R) = -0.25 \pm 0.07$. This radial range covers the range for which M32 possesses no signs of optical or near-infrared color gradients. O'Connell (1992) presented an ultraviolet color gradient in M32 "bluening" outwards. This was interpreted as an age gradient, in which the center is the younger. Silva & Elston (1994) concluded that the close-to-zero color gradients in the near-infrared were a sign of constant age and metallicity with radius, and this interpretation was found to be in agreement with Peletier (1993). The indication by Hardy *et al.* of a nearly zero age gradient seems difficult to explain in view of their observed metallicity gradient *and* the zero optical and near-infrared color gradients presented in the literature, unless some characteristic other than age varies with radius. Furthermore, the state-of-the-art stellar population models of Worthey (1994) (hereafter referred to as Worthey), which involve the presence of ABG stars, are not able to describe the combination of these observed properties. The models predict that gradients in Mg_2, $B-I$, and $\bar{m}_I$ introduced by the metallicity gradient observed by Hardy *et al.* could be erased by an age gradient, the galaxy being youngest at the center. The evidence of a gradient in Mg_2, but the lack of such in broad-band colors, indicates that at least two parameters are required in order to describe M32. One of the two parameters is very likely metallicity. A variation in age cannot be excluded, and the ultraviolet studies of Dorman *et al.* 1995 (discussed below) suggest additional parameters such as a presence of extreme horizontal branch (EHB) stars and/or post asymptotic giant branch (PAGB) stars. A presence of such "blue" stars may be adopted as a possible third parameter of the stellar population, in addition to metallicity and age. Faber *et al.* (1992) divided the parameter sequence into light-element abundance, iron-peak abundance, and probably age.

The increase in the luminosity fluctuations in the B and I-band towards the center of M32 is not in conflict with the presence of more than one type of stars contributing differently to each bandpass. (A similar but a much less significant change towards the center of NGC 3379 may be seen in Fig. 3 of ST). We tentatively interpret the upturn in I as yet another indication of the (likely centrally concentrated) intermediate-age AGB population in M32, whereas the upturn in B probably is caused by an associated population of putative "blue" stars. Regarding the variation in the B-band luminosity fluctuations of M32, the work by Dorman *et al.* (1995) on the ultraviolet (UV) upturn phenomenon in elliptical galaxies is of interest. Dorman *et al.* found that for galaxies with "normal" UV

excess a considerable part of the HB must be comprised by EHB stars in order to explain the UV upturn. For M32, which is relatively faint in the UV, a presence of EHB stars or a PAGB sequence can supply the observed flux at those short wavelengths. The UV properties of M32 were found to be consistent with a solar abundance, intermediate-age population. Worthey (1993) calculated U and B-band luminosity fluctuations for populations with differing horizontal branch morphologies. In Fig. 4(a) we compare these models, which involve a "Red Clump" HB and a hotter "Extended" HB, respectively, with our observations of B-band luminosity fluctuations. (The extended HB and the blue HB in Worthey [1993] differ only by a few hundredths of a magnitude in $\bar{B}$). Both of the models with differing HBs are plotted for a population of 8 Gyr and [Fe/H] = 0.0. This choice is merely an example motivated by the studies referenced in this paper; other of the hot HB models in Worthey (1993) with different age/metallicity values would fit the current dataset equally well. Fig. 4(a) indicates that there is a need for a hot ($\log T_e > 3.7$) HB population in the models in order to describe the observations. This supports Worthey's (1993) suggestion that hot HBs are readily detectable from SBF measurements. As stressed by Worthey, HST observations could unveil such luminous stars, and with their identification it should be possible to make constraints on the strength of a hot HB. Far-UV HST observations of the M32 nucleus have revealed 10 individual stars (Bertola *et al.* 1995). Due to the low number of UV-bright stars the authors do not make any statistically significant interpretation. Superluminous PAGB stars could possibly give an additional contribution to the luminosity fluctuations.

The radial variation in the B-band luminosity fluctuations seen in Fig. 4(a) may be caused by a variation in the HB morphology. Yet another parameter that could explaine the observed properties of the stellar population is the balance of dwarf stars versus giant stars (Rose 1994). Since the SBF signal is particularly sensitive to the brightest stars in the population (in the bandpass that one is considering), one may expect that a varying ratio of giants to dwarfs would be reflected in a radial variation in $\bar{m}$. Also, Rose finds indications

Fig. 4.— Observed B and I-band fluctuation magnitudes for M32 as a function of radius: $\bar{m}_B$ ($*$), $\bar{m}_I$ ($\diamond$), and color $\bar{m}_B - \bar{m}_I$ ($\triangle$). The size of the symbols corresponds to the statistical error ~ 0.04 mag. Superposed are the stellar population models of Worthey (1993, 1994) shifted to a distance modulus of $\bar{m}_I - \bar{M}_I = 24.51$ (Pahre & Mould 1994). The B-band model predictions involving red clump and extended HBs are plotted for 8 Gyr solar abundance populations (Worthey 1993). The I-band predictions involve red clump HBs and are plotted for an 8 Gyr population and metallicities [Fe/H] = 0.0 and [Fe/H] = −0.25, respectively (Worthey 1994). Note, the models represent single-age single-metallicity burst populations.

of the existence of an intermediate-age population in M32.

In Fig. 4(b) we have presented our measurements of $\bar{m}_I$. At these redder wavelengths (I relative to B) the luminosity fluctuations are dominated by the cooler RGB (and AGB) stars. The predictions of Worthey (1994), which involve a red clump HB, are plotted for an 8 Gyr population (cf., Jones & Worthey 1995 below) and two metallicities [Fe/H] = 0.0 and [Fe/H] = −0.25. The model predictions for $\bar{m}_I$ are close to the observed range and are not inconsistent with the general idea that M32 possess an intermediate-age population. The upturn in $\bar{m}_I$ with increasing distance from the center may be explained by a decrease in metallicity as indicated by the models. However, a variation in parameters other than metallicity and age cannot be excluded. Freedman (1989) sets a lower limit to the mean metallicity of -0.5 ± 0.2 for the field 2′ south of the M32 nucleus. The fact that this was a lower limit was mainly due to incompleteness in V, introducing a lack in redder stars and thereby an underestimate of the color and metallicity. Freedman inferred an intrinsic range in metallicity of 0.6 dex for the stars in this field. The fluctuation color $\bar{m}_B - \bar{m}_I$ is shown in Fig. 4(c). The color has the average value $\bar{m}_B - \bar{m}_I = 4.90 \pm 0.05$ and tends to become slightly bluer toward the center and outward in the galaxy. Note that the data are being compared to models which are of single-age and single-metallicity. In reality, M32 probably has a range of metallicity and at least two ages: an older (> 10 Gyr) population and an intermediate-age (4–8 Gyr) population (e.g., Freedman 1989, 1992b). Different bandpasses, such as B and I, will be sensitive to populations with different ages and metallicities.

In Fig. 5 we have plotted the gradient vector (ΔIndex/Δ log(age), ΔIndex/Δ[Fe/H]), where the model index (Worthey) is viewed as a surface on the parameter space (log(age), [Fe/H]) (see ST for details). Fig. 5 shows how a few of the available indices change as a function of small changes in age and metallicity around an age of 4.9 Gyr (the geometric mean of 3 and 8 Gyr) and [Fe/H] = 0.0. The plot indicates that the indices $B - I$, Fe_{5270}, $\bar{I}$, $\bar{B}$, and $\bar{U}$ do not give significantly different information regarding small changes in age and metallicity. H_β varies mainly as a function of age, and the iron index Fe_{5270} is mainly sensitive to metallicity. The new Balmer line index $\mathrm{H}_{\gamma\mathrm{HR}}$ (not available in Worthey) found by Jones & Worthey (1995) to break the degeneracy between age and metallicity was plotted against the iron feature Fe_{4668} in their Fig. 2. The associated data point obtained for the M32 nucleus was found to lie near the 7 Gyr model with metallicity slightly above solar. As emphasized by Jones & Worthey this is in agreement with the

Fig. 5.— Stellar population model indices as a function of changes in age and metallicity around 4.9 Gyr and [Fe/H] = 0.0 (Worthey 1994), see text.

studies of others. However, their presented model grid was based on a red clump HB alone, and a contribution to the Balmer line model indices from possible hotter HB stars may alter (i.e., increase) the age of M32 slightly. From U-band observations of luminosity fluctuations in M32 Worthey (1993) argued that $\sim 9\%$ of the population has extended or blue HBs.

We now discuss the possibility that the SBF variations seen in M32 could be caused by patches of dust and/or gas. Besides dust patches, a diffuse distribution of dust may cause a color gradient due to differential extinction, which may be a possible factor in addition to stellar populations variations (Witt *et al.* 1992). However, neither M32 nor NGC 3379 were detected at 60μm and 100μm in IRAS data (Knapp *et al.* 1989), and no dust patches are evident in the optical colors. Regarding dust and gas in ellipticals, see also Goudfrooij *et al.* (1995) and Kormendy *et al.* (1994). Silva & Elston (1994) discussed the radial age and metallicity degeneracy in elliptical galaxies. One of the advantages of observing in the near-infrared that they emphasized was the ability to trace the stellar population in the presence of dust, due to the much less reddened near-infrared colors contrary to the optical.

As emphasized earlier, when the measurements of SBF are used to infer relative distances of galaxies, say M32 and NGC 3379, any differences in the underlying stellar population of the galaxies must be calibrated for. The importance of this is explicit if NGC 3379 should possess a different amount of young, bright AGB stars. In the following we discuss to what extent the AGB stars influence the luminosity fluctuations in M32. A lower limit from AGB stars to the SBF signal $\bar{m}_I$ was estimated in the following way. Freedman (1989) presented an I vs $(V-I)$ color-magnitude diagram for stars in a field $\sim 2'$ to the south of the M32 nucleus (see Fig. 9 therein). Freedman found two breaks in the I-band giant star luminosity function. If the fainter break $I = 20.45$ (which corresponds to $M_I \sim -4$) was adopted as the tip of the first red giant branch (TRGB) (i.e., the onset of the brightest RGB stars), the interpretation involved a population of AGB stars in M32 significantly younger than those found in galactic globular clusters. Based on both observations and simulations Madore & Freedman (1995) have shown that for a metal-poor population ($-2.2 < [\mathrm{Fe/H}] < -0.7$) the TRGB is indeed the upper limit of the brightest RGB stars (see also Lee *et al.* 1993). Adopting all stars brighter than the TRGB as AGB stars we have calculated the flux $\bar{f}_{\mathrm{AGB}} = \sum n_{\mathrm{AGB}} f_{\mathrm{AGB}}^2 / \bar{g}$, where the sum was taken over the area of the galaxy field under consideration. Here $n_{\mathrm{AGB}} = 105$, and f_{AGB} are read from Fig. 9(b) in Freedman (1989). The average galaxy flux $\bar{g}$ at $R \sim 2'$ was estimated by an extrapolation of our galaxy profile. If the adopted magnitude for the TRGB is $I = 20.45$ then $\bar{f}_{\mathrm{AGB}}$ constitutes $\sim 15\%$ of the SBF signal $\bar{f}$. Alternatively, Freedman adopted $I = 20.15$ as the TRGB. This involved the interpretation that M32 should be about 100 kpc closer than M31 and the age of most of the M32 stars comparable to the ages of galactic globular clusters. In this case $\bar{f}_{\mathrm{AGB}}$ constitutes $\sim 10\%$ of the SBF signal. The contribution

from AGB stars to the fluctuation signal is not insignificant, but the contribution effects the distance estimate by at most $\sim 7\%$. As emphasized by Freedman, the inferred AGB population is very sensitive to the choice of the TRGB. Observations in the K-band of a $20'' \times 18''$ field also $\sim 2'$ south of the M32 nucleus (Freedman 1992b) showed that the resolved AGB population contributes approximately 10% of the integrated light. We have used this value to estimate that $\sim 30\%$ of the SBF signal in K would be from the AGB stars. For reference, Luppino & Tonry (1993) find no gradient in K' SBF measurements in M32 within $R \simeq 48''$.

An estimate of the contribution to the fluctuation signal from the AGB stars close to the center may be obtained from Davidge & Nieto (1992). (We here ignore the possibility that an unknown fraction of their studied population of AGB stars may be spurious objects due to luminosity fluctuations, see the discussion in Sec. 3). Davidge & Nieto presented an I vs $I - 1\mu$m color-magnitude diagram of a central $65'' \times 110''$ field of M32. The photometric properties of the brightest stars were presented as luminosity functions for three distinct annuli in the region $5''.5 < R < 27''.5$. The slope of the luminosity functions was found to be $\mathrm{dlog}\, N(m)/\mathrm{d}m \sim 1.5$. Based on this we estimate the contribution from AGB stars by integrating the luminosity functions instead of the simple sum above. The integral is very sensitive to the choice of the adopted TRGB, in the way that it is dominated by the large number of stars at the faint end of the magnitude bin over which the integral is performed. The expected contribution from AGB stars was found to be a factor of 4 to 6 times larger for the field near the center than for the field at the distance of $2'$ from the center. This estimate should only be regarded as a tentative upper limit.

The average value of the I-band luminosity fluctuations in M32 presented here is $\bar{m}_I = 22.78 \pm 0.04$, which is close to that found by Tonry (1991) $\bar{m}_I = 22.81 \pm 0.05$. We have calibrated the possible differencies in the stellar populations constituting M32 and NGC 3379 by adopting the SBF magnitude $\bar{m}$ for NGC 3379 at that particular local color of the surface brightness which matched the integrated color of M32. The numbers are $\bar{m}_{I,\mathrm{M32}} = 22.78 \pm 0.04$ and $\bar{m}_{I,\mathrm{NGC3379}} = 28.64 \pm 0.04$ at $(B - I) = 1.98$, i.e., at the integrated color of M32 after de-reddening. This implies $d_{\mathrm{NGC3379}} = (14.9 \pm 0.4) \times d_{\mathrm{M32}}$. If we adopt $d_{\mathrm{M32}} = 0.77$ Mpc (Freedman & Madore 1990) we find $d_{\mathrm{NGC3379}} = 11.4 \pm 0.6$ Mpc, which within the errors is equal to the optical Cephied distance of 11.6 ± 0.8 Mpc to the Leo Group obtained by Tanvir *et al.* (1995). A determination of the distance to M31 and M32 based on infrared observations of Cepheids yields 0.71 Mpc (Welch *et al.* 1986), and based on observations of RR Lyraes Pritchet & van den Bergh (1988) find a distance of 0.70 Mpc. With these distances for M32 we find $d_{\mathrm{NGC3379}} = 10.5 \pm 0.6$ Mpc. I-band SBF distance moduli were presented in Pahre & Mould (1994), which implied that $d_{\mathrm{NGC3379}} = (12.0 \pm 0.7) \times d_{\mathrm{M32}}$. It should be noted that comparing galaxies at different

galactic latitude is likely to introduce systematic errors due to the adopted correction for foreground reddening (Sec. 2.1).

Unlike broad-band colors and spectral indices, the luminosity fluctuations give information about the distance to the target galaxy, and an investigation of the SBF of a nearby galaxy in terms of its stellar population is absolutely essential for the distance estimates of more distant galaxies. We have presented the radial behavior of the SBF in our closest elliptical galaxy M32. Whereas data presented in the literature does not indicate radial variations in the optical and near-IR broad-band colors, we find a systematic variation in the I and B-band luminosity fluctuations. This indicates that SBF trace a radial variation in the stellar population, which is not traced by broad-band colors. Generally, measurements of luminosity fluctuations are not able to disentangle the degeneracy of age and metallicity. Whereas this is in favour of the SBF as a distance indicator, the SBF variation seen in M32 demonstrates that the calibration of fluctuation magnitude against broad-band colour is not unique. The cause of the change in the stellar population remains unsolved. However, we find that our observations are not in conflict with the indications of others, namely that M32 does possess a population of bright intermediate-age stars. Further observations of M32 should be combined with simulations of seeing and crowding effects to facilitate a reliable discrimination between individual bright stars and spurious objects due to luminosity fluctuations. The observed B-band luminosity fluctuations indicate that M32 carries a significant amount of hot (e.g. horizontal branch) stars. From HST UV observations it may be possible to determine the presence of the stellar populations that give rise to this "blue" light.

We wish to thank P. B. Stetson for the benefits of using his photometry package DAOPHOT II, and we thank an anonymous referee for constructive criticism of the manuscript. MS acknowledges the dedicated and joyful support from the staff at the NOT, and financial support from the University of Aarhus Faculty of Science.

REFERENCES

Ajhar, E. A., & Tonry, J. L. 1994, ApJ, 429, 557

Bahcall, J. N., & Soneira, R. M. 1980, ApJS, 44, 73

Bertola, F., *et al.* 1995, ApJ, 438, 680

Burstein, D., Faber, S. M., Gaskell, C. M., & Krumm, N. 1984, ApJ, 287, 586

Burstein, D., & Heiles, C. 1984, ApJS, 54, 33

Burstein, D., Davies, R. L., Dressler, A., Faber, S. M., Stone, R. P. S., Lynden-Bell, D., Terlevich, R. J., & Wegner, G. 1987, ApJS, 64, 601 (B87)

Caon, N., Capaccioli, M., & D'Onofrio, M. 1993, MNRAS, 265, 1013

Capaccioli, M., & de Vaucouleurs, G. 1983, ApJS, 52, 465

Cardelli, J. A., Clayton, G. C., & Mathis, J. S. 1989, ApJ, 345, 245

de Vaucouleurs, G., de Vaucouleurs, A., Corwin, H. G., Buta, R. J., Paturel, G., & Fouqué, P. 1991, Third Reference Catalogue of Bright Galaxies (Springer, New York)

Davidge, T. J. 1991, AJ, 101, 884

Davidge, T. J., & Jones, J. H. 1992, AJ, 104, 1365

Davidge, T. J., & Nieto, J.-L. 1992, ApJ, 391, L13

Davies, R. L., Sadler, E. M., & Peletier, R. F. 1993, MNRAS, 262, 650

Davis, L. E. 1995, private communication

DePoy, D. L., Terndrup, D. M., Frogel, J. A., Atwood, B., & Blum, R. 1993, AJ, 105, 2121

Dorman, B., O'Connell, R. W., & Rood, R. T. 1995, ApJ (in press)

Elston, R., & Silva, D. R. 1992, AJ, 104, 1360

Faber, S. M. 1973, ApJ, 179, 423

Faber, S. M., Trager, S. C., Gonzalez, J. J., & Worthey G. 1995, in Stellar Populations, IAU Symposium No. 164, edited by P. C. van der Kruit and G. Gilmore (Dordrecht: Kluwer), 249

Ferguson, H. C., & Binggeli, B. 1994, A&AR, 6, 67

Freedman, W. L. 1989, AJ, 98, 1285

Freedman, W. L. 1992a, in The Stellar Population of Galaxies, IAU Symposium No. 149, edited by B. Barbuy and A. Renzini (Dordrecht: Kluwer), 169

Freedman, W. L. 1992b, AJ, 104, 1349

Freedman, W. L., & Madore, B. F. 1990, ApJ, 365, 186

Gregg, M. D. 1989, ApJS, 69, 217 (G89)

Goudfrooij, P., & de Jong, T. 1995, A&A, 298, 784

Hardy, E., Couture, J., Couture, C., & Joncas, G. 1994, AJ, 107, 195

Harris, W. E. 1991, ARA&A, 29, 543

Hodge, P. W. 1981, in Atlas of the Andromeda Galaxy (University of Washington, Seattle)

Jones, L. A., & Worthey, G. 1995, ApJ, 446, L31

King, D. L. 1985, in Atmospheric Extinction at the Roque de los Muchachos Observatory, La Palma, RGO/La Palma Technical Note No. 31

Knapp, G. R., Guhathakurta, P., Kim, D.-W., & Jura, M. 1989, ApJS, 70, 329

Kormendy, J. 1985, ApJ, 295, 73

Kormendy, J., *et al.* 1994, in ESO/OHP Workshop on Dwarf Galaxies, edited by G. Meylan and P. Prugniel (Garching: ESO), 147

Landolt, A. U. 1992, AJ, 104, 340

Lee, M. G., Freedman, W. L., & Madore, B. F. 1993, ApJ, 417, 553

Lilly, S. J., Cowie, L. L., & Gardner, J. P. 1991, ApJ, 369, 79

Luppino, G. A., & Tonry, J. L. 1993, ApJ, 410, 81

Madore, B. F., & Freedman, W. L. 1995, AJ109, 1645

Majewski, S. R., Kron, R. G., Koo, D. C., & Bershady, M. A. 1994, PASP, 106, 1258

Michard, R., & Nieto, J.-L. 1991, A&A, 243, L17

Morrison, L. V. 1994, private communication

O'Connell, R. W. 1980, ApJ, 236, 430

O'Connell, R. W. 1992, in The Stellar Population of Galaxies, IAU Symposium No. 149, edited by B. Barbuy and A. Renzini (Dordrecht: Kluwer), 233

Pahre, M. A., & Mould, J. R. 1994, ApJ, 433, 567

Peletier, R. F., *et al.* 1990, AJ, 100, 1091

Peletier, R. F. 1992, in ESO Conference and Workshop Proceedings 45, edited by I. J. Danziger, W. W. Zeilinger, and K. Kjär, Structure, Dynamics and Chemical Evolution of Elliptical Galaxies, 409

Peletier, R. F. 1993, A&A, 271, 51 (P93)

Press, W. H., Flannery, B. P., Teukolsky, S. A., & Vetterling W. T. 1992, in Numerical recipes in C. – 2nd ed. (Cambridge University Press), 553

Pritchet, C. J., & van den Bergh, S. 1988, ApJ, 344, 704

Racine, R. 1991, AJ, 101, 865

Ratnatunga, K. U., & Bahcall, J. N. 1985, ApJS, 59, 63

Reed, L. G., Harris, G. L. H., & Harris, W. E. 1994, AJ, 107, 555

Renzini, A. 1986, in Stellar Populations, edited by C. A. Norman, A. Renzini, and M. Tosi, (Cambridge University Press, Cambridge), 213

Rose, J. A. 1985, AJ, 90, 1927

Rose, J. A. 1994, AJ, 107, 206

Sandage, A., & Visvanathan, N. 1978, ApJ, 223, 707 (SV78)

Silva, D. R., & Elston, R. 1994, ApJ, 428, 511

Sodemann, M., & Thomsen, B. 1994, A&A, 292, 425

Sodemann, M., & Thomsen, B. 1995, AJ, 110, 179 (ST)

Stetson, P. B. 1987, PASP, 99, 191

Stetson, P. B., & Harris, W. E. 1988, AJ, 96, 909

Tanvir, N. R., Shanks, T., Ferguson, H. C., & Robinson, D. R. T. 1995, NATURE, 377, 27

Thomsen, B., & Frandsen, S. 1983, AJ, 88, 789

Thomsen, B., & Sodemann, M. 1995 (in preparation)

Tonry, J. L. 1984, ApJ, 283, L27

Tonry, J. L. 1991, ApJ, 373, L1

Tonry, J. L., Ajhar, E. A., & Luppino, G. A. 1990, AJ, 100, 1416

Tonry, J., & Schneider, D. P. 1988, AJ, 96, 807

Tyson, J. A. 1988, AJ, 96, 1

Welch, D. L., McAlary, C. W., McLaren, R. A., & Madore, B. F. 1986, ApJ, 305, 583

Witt, A. N., Thronson, H. A., Capuano, J. M. 1992, ApJ, 393, 611

Worthey, G. 1993, ApJ, 415, L91

Worthey, G. 1994, ApJS, 95, 107 (Worthey)

This preprint was prepared with the AAS LaTeX macros v3.0.

The following is a list of Table captions for the paper "Variation in the Surface Brightness Fluctuations of M32".

Notes to Table 1.– Column 1 gives the references Sandage & Visvanathan 1978 (SV78), Burstein *et al.* 1987 (B87), Peletier 1993 (P93), and Gregg 1989 (G89), Columns 2 ($\log A$) and 3 ($A/2$) give the logarithm of the adopted aperture in $0''.1$ and the corresponding radius in arcsec, Columns 4 (B) and 5 (I) are the integrated broad-band B and I magnitudes within R, and Column 6 ($B-I$) is the integrated color $B-I$. For P93, $B-I$ is the median of the flat color profile between $1''.5$ and $42''$. For G89, who had corrected for reddening, we adopted $\mathrm{E}(B-I)=0.17$. Then, none of the numbers given in Table 1 have been corrected for reddening. Typical statistical errors for the individual passbands are 0.03.

Notes to Table 2.– For each annulus of the galaxy the following is tabulated. Column 1 (R) is the geometric mean radius in arcsec, Column 2 ($B-I$) is the reddening-corrected broad-band surface brightness color at R, Columns 3 and 5 ($P_0^{I,B}$), and 4 and 6 ($P_1^{I,B}$) are the measured power in ADUs for SBF and white noise respectively during 25 s for I and 90 s for B, Columns 7 and 8 ($\bar{m}'_{I,B}$) are P_0^I and P_0^B expressed in magnitudes. In Column 9 and 10 ($\bar{m}_{I,B}$) we give the fluctuation magnitudes after the adjustment for M31 have been applied (Sec. 3). All magnitudes $\bar{m}'$ and $\bar{m}$ have been corrected for reddening according to Sec. 2.1.

TABLE 1. Comparison of photometry for M32.

Reference	$\log A$	$A/2$	B	I	$B-I$
SV78	1.15	42.4	9.77	–	–
this paper	do	do	9.75	7.63	2.12
B87	1.00	30.0	10.02	–	–
this paper	do	do	9.97	7.84	2.13
P93	–	–	–	–	2.08
G89	–	–	–	–	2.15

Notes to Table 1.

Column 1 gives the references Sandage & Visvanathan 1978 (SV78), Burstein *et al.* 1987 (B87), Peletier 1993 (P93), and Gregg 1989 (G89), Columns 2 ($\log A$) and 3 ($A/2$) give the logarithm of the adopted aperture in 0.″1 and the corresponding radius in arcsec, Columns 4 (B) and 5 (I) are the integrated broad-band B and I magnitudes within R, and Column 6 ($B-I$) is the integrated color $B-I$. For P93, $B-I$ is the median of the flat color profile between 1.″5 and 42″. For G89, who had corrected for reddening, we adopted $E(B-I) = 0.17$. Then, none of the numbers given in Table 1 have been corrected for reddening. Typical statistical errors for the individual passbands are 0.03.

TABLE 2. Data for radial SBF analysis of M32.

R	$B-I$	P_0^I	P_1^I	P_0^B	P_1^B	$\bar{m}_I^{'}$	$\bar{m}_B^{'}$	$\bar{m}_I$	$\bar{m}_B$
11.6	1.86	37.0	0.05	5.74	0.04	22.78	26.73	22.78	26.74
20.3	1.94	34.3	0.05	4.87	0.04	22.86	26.91	22.85	26.93
29.1	1.96	34.7	0.06	5.30	0.04	22.85	26.82	22.83	26.86
37.8	1.95	37.3	0.07	6.06	0.05	22.78	26.67	22.74	26.71
46.6	1.95	38.0	0.08	6.51	0.06	22.76	26.60	22.71	26.65

Notes to Table 2.

For each annulus of the galaxy the following is tabulated. Column 1 (R) is the geometric mean radius in arcsec, Column 2 ($B-I$) is the reddening-corrected broad-band surface brightness color at R, Columns 3 and 5 ($P_0^{I,B}$), and 4 and 6 ($P_1^{I,B}$) are the measured power in ADUs for SBF and white noise respectively during 25 s for I and 90 s for B, Columns 7 and 8 ($\bar{m}_{I,B}^{'}$) are P_0^I and P_0^B expressed in magnitudes. In Column 9 and 10 ($\bar{m}_{I,B}$) we give the fluctuation magnitudes after the adjustment for M31 have been applied (Sec. 3). All magnitudes $\bar{m}^{'}$ and $\bar{m}$ have been corrected for reddening according to Sec. 2.1.

The following is a list of Figure captions for the paper "Variation in the Surface Brightness Fluctuations of M32".

Fig. 1.– I-band growth curve for one bright relatively isolated calibrating star in M92. This clearly demonstrates the effects of light scattered from the central parts of the stellar object into the wings. Plotted is the integrated magnitude within 12 different radii subtracted from the integrated magnitude within the innermost aperture of radius 2.″6. The standard aperture adopted for aperture correction in the I-band had a radius of 5.″2 when dealing with the photometry of the PSF and 21″ when dealing with the photometry of the galaxy. Neighboring stars were masked out in order to determine a background not too affected by point sources. The inner and outer sky annuli were 38″ and 45″, respectively. The PHOTOMETRY routine of DAOPHOT II was applied (Stetson 1987).

Fig. 2.– Histogram of detected objects in the original I-band residual image (full line), and of detected objects in the simulated image where the luminosity function equals a delta function at $I = \bar{m}_I = 22.78$ (dashed line). All detected objects with SIGMA larger than 0.08 have been eliminated, see text. The data are plotted in 0.1 magnitude bins. The vertical line represents the average magnitude of a fluctuation star with $I = \bar{m}_I$. The gap between $I \sim 19.5$, where the bulk of objects is found, and $I = 22.78$ is explained qualitatively in the text. Data are 100% complete for $I < 19.5$

Fig. 3.– Power spectra of normalized luminosity fluctuations, one for each annulus in I (ADU per 25 s) and B (ADU per 90 s), respectively. Also shown is the sum of the power P_0 times $|OTF(\omega)|^2$ plus the level of white noise P_1. The luminosity fluctuation signal $\bar{f}$ is derived from the power spectrum with wavenumbers in the range $25 \leq \omega \leq 130$, corresponding to the central few arcsec ($\sim 1'' - 7''$) of the PSF.

Fig. 4.– Observed B and I-band fluctuation magnitudes for M32 as a function of radius: $\bar{m}_B$ ($*$), $\bar{m}_I$ ($\diamond$), and color $\bar{m}_B - \bar{m}_I$ ($\triangle$). The size of the symbols corresponds to the statistical error ~ 0.04 mag. Superposed are the stellar population models of Worthey (1993, 1994) shifted to a distance modulus of $\bar{m}_I - \bar{M}_I = 24.51$ (Pahre & Mould 1994). The B-band model predictions involving red clump and extended HBs are plotted for 8 Gyr solar abundance populations (Worthey 1993). The I-band predictions involve red clump HBs and are plotted for an 8 Gyr population and metallicities [Fe/H] = 0.0 and [Fe/H] = −0.25, respectively (Worthey 1994). Note, the models represent single-age single-metallicity burst populations.

Fig. 5.– Stellar population model indices as a function of changes in age and metallicity around 4.9 Gyr and [Fe/H] = 0.0 (Worthey 1994), see text.

Figure 1

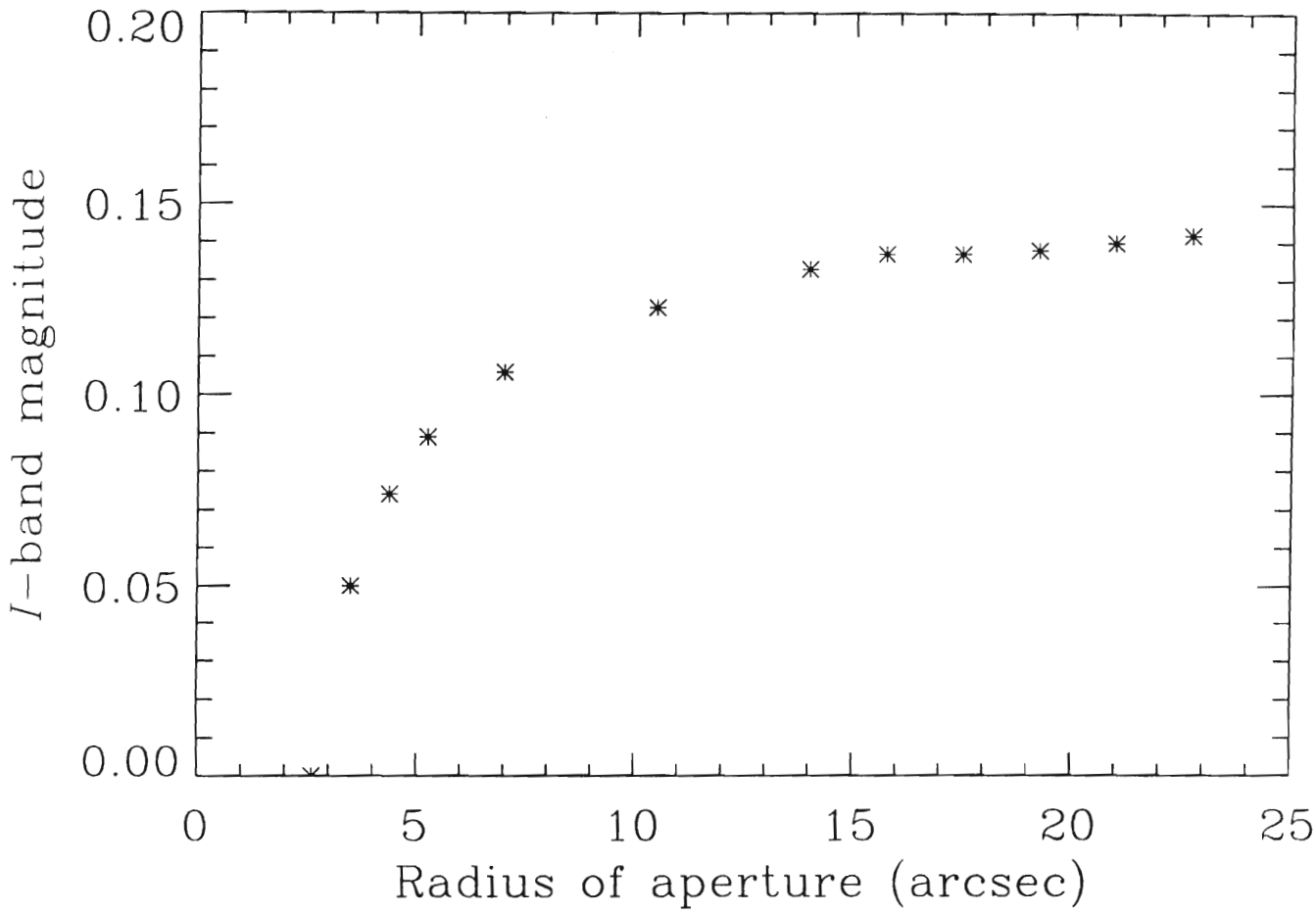
0.20
0.15
0.10
0.05
0.00
I−band magnitude
0
5
10
15
20
25
Radius of aperture (arcsec)

Figure 2

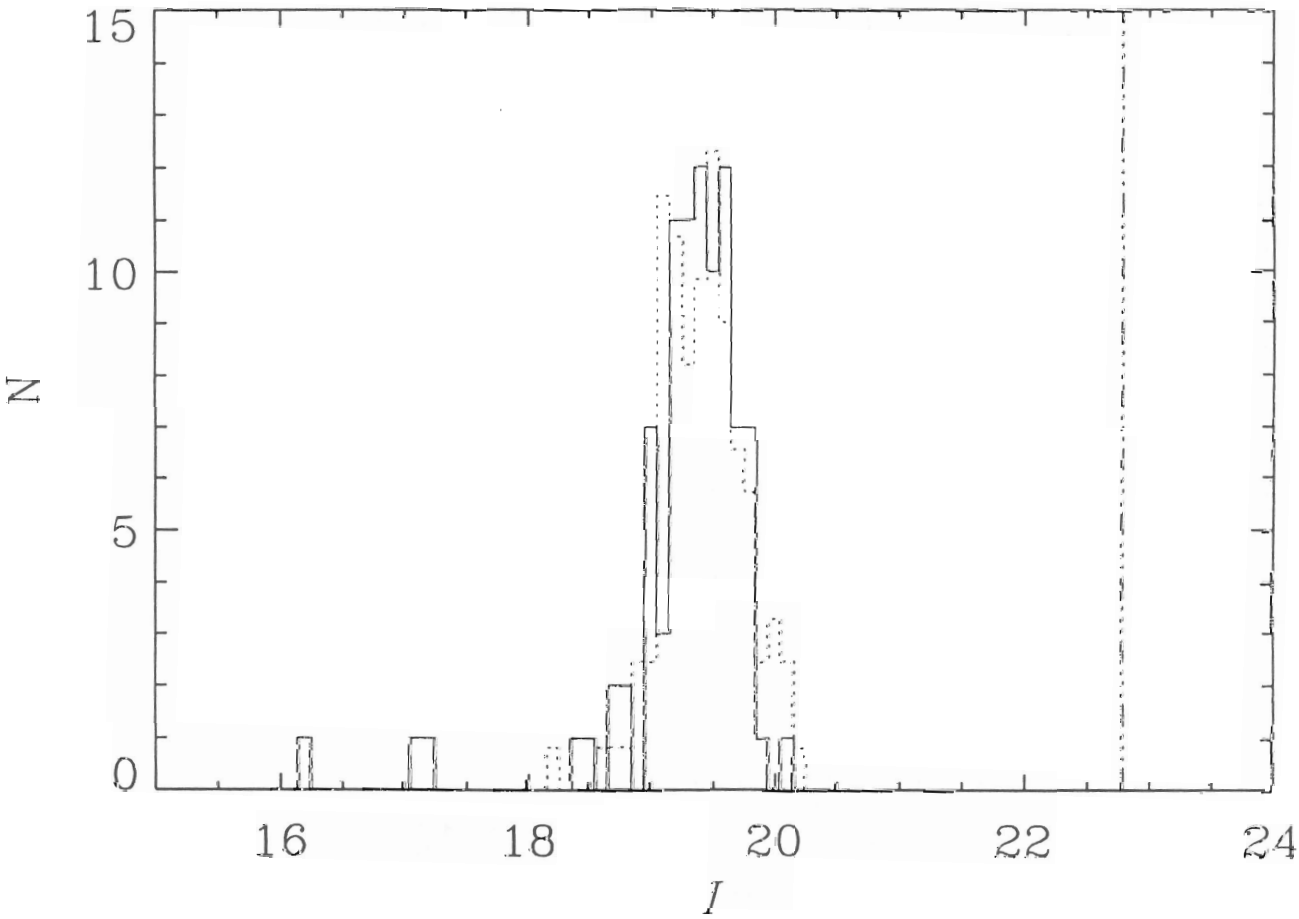

Figure 3

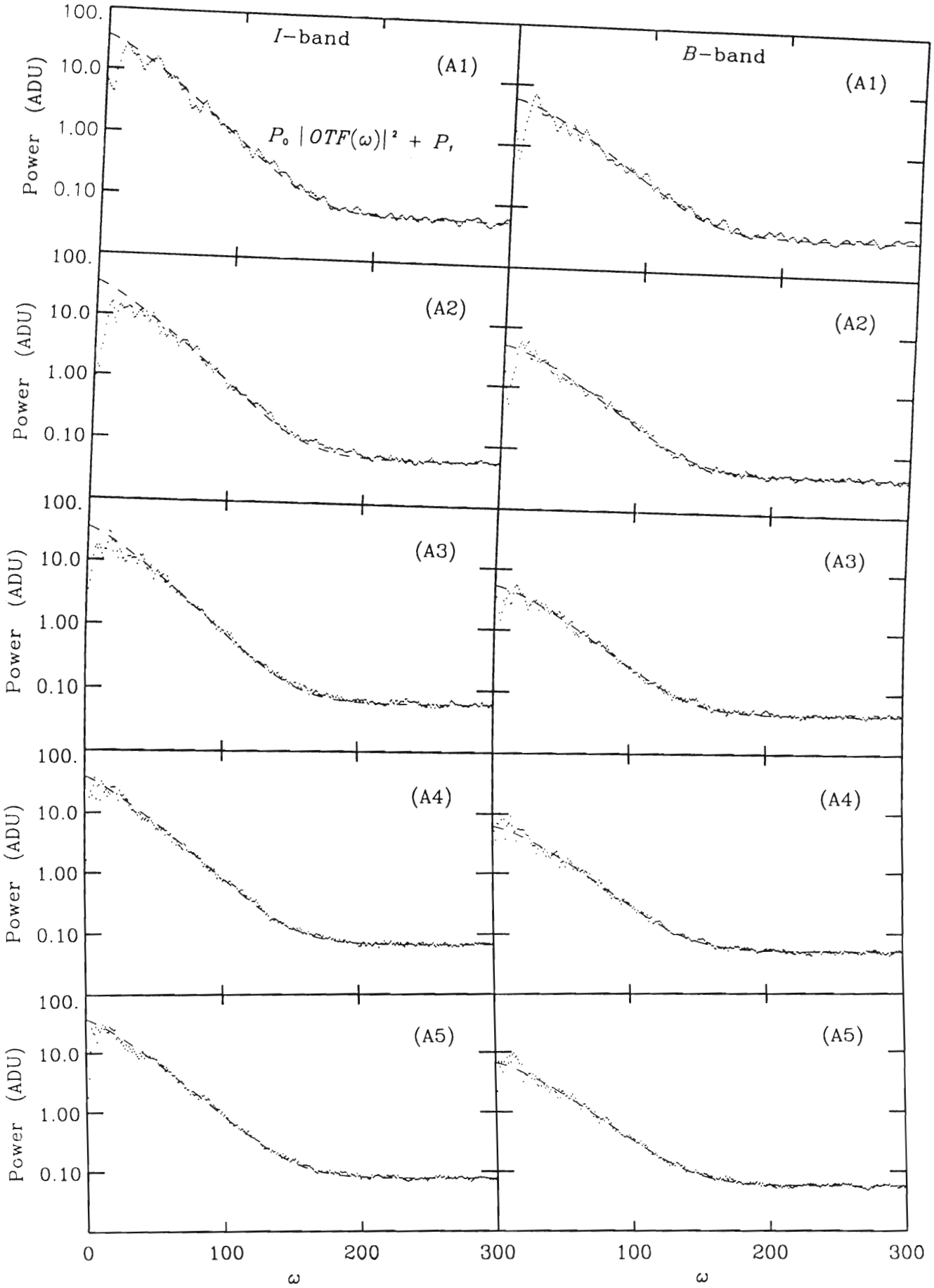
I−band
B−band
(A1)
(A2)
(A3)
(A4)
(A5)
$P_0 \, |OTF(\omega)|^2 + P_r$
Power (ADU)
100.
10.0
1.00
0.10
0
100
200
300
ω

Figure 4

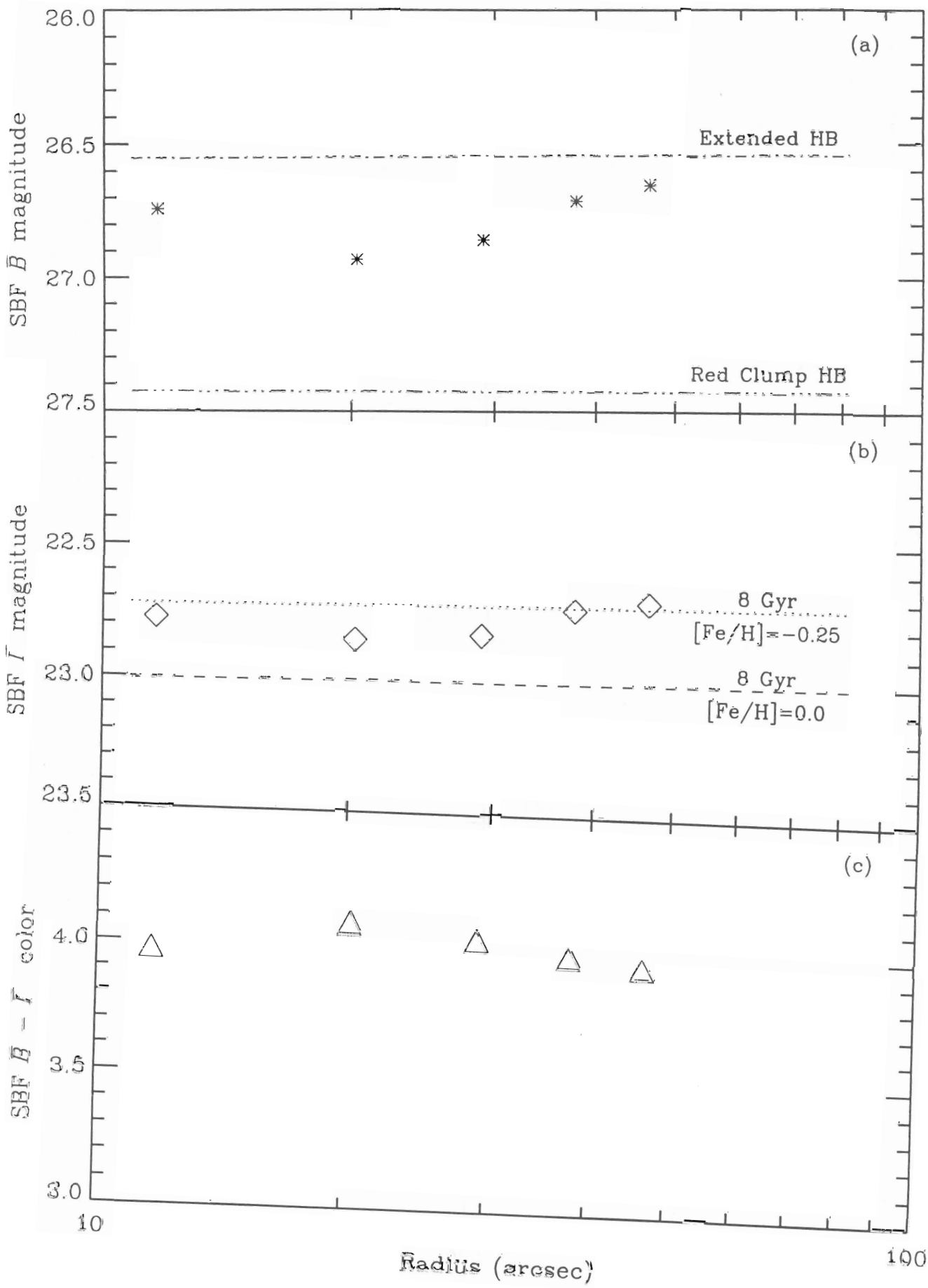
(a)
Extended HB
Red Clump HB
SBF $\bar{B}$ magnitude
26.0
26.5
27.0
27.5
(b)
8 Gyr
[Fe/H]=−0.25
8 Gyr
[Fe/H]=0.0
SBF $\bar{I}$ magnitude
22.5
23.0
23.5
(c)
SBF $\bar{B}-\bar{I}$ color
4.0
3.5
3.0
10
100
Radius (arcsec)

Figure 5

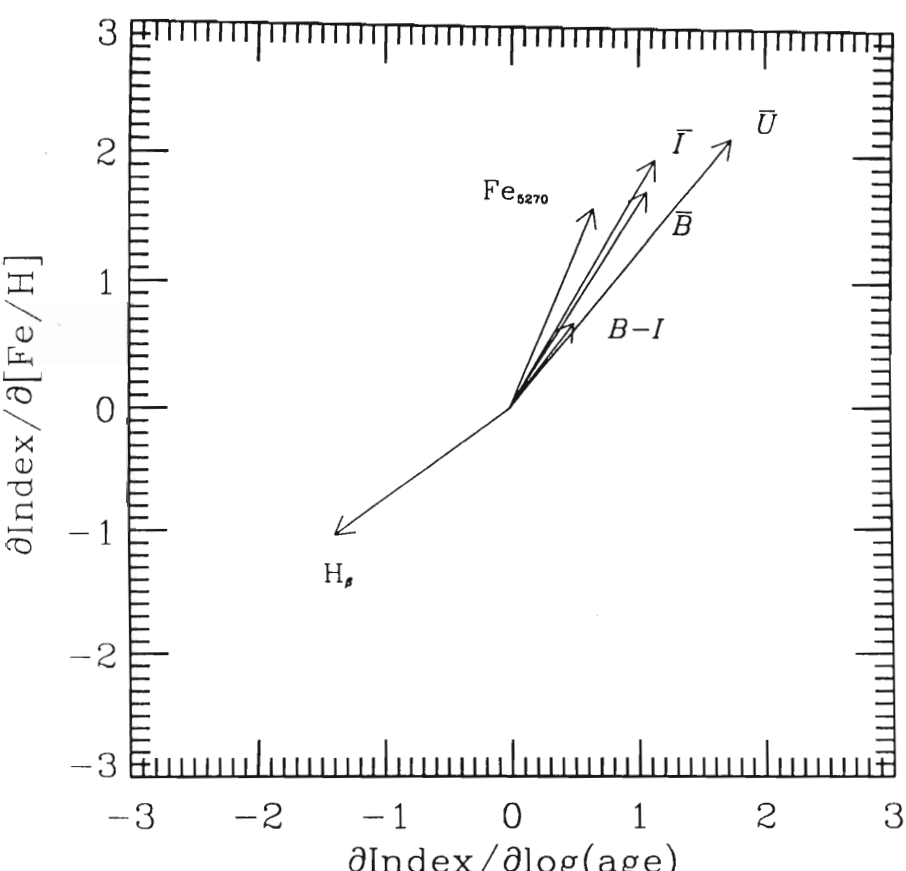
3
2
1
0
−1
−2
−3
−3
−2
−1
0
1
2
3
∂Index/∂[Fe/H]
∂Index/∂log(age)
$\bar{U}$
$\bar{I}$
$\bar{B}$
$B-I$
Fe_{5270}
H_β